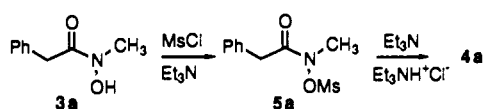
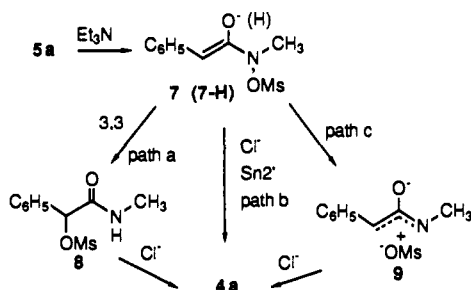


Scheme I

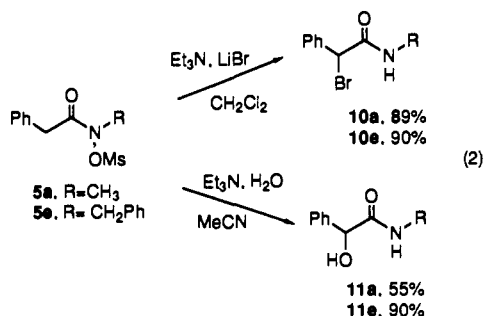


Scheme II



better nucleophile.¹² This result shows that S_N2' attack on enol 7-H is not rate determining (second step of path b). Furthermore, the formation of enol 7-H (first step of path b) is governed by a proton-transfer equilibrium, not by irreversible proton removal as is found (*vide infra*). Path b is thus discounted since neither step is consonant with the observed behavior.

The results from the substituent effect experiments and the requirement of a conjugating group at C-2 suggest that proton removal by base is occurring in the rate-determining step. The lack of deuterium incorporation means that proton removal is not reversible. The greater reactivity of triflate over mesylate might be attributed to an increase in acidity of the α -proton from the greater electron-withdrawing ability of the triflate group. A mechanism involving conversion of 5a to enolate 7 followed by formation of ion pair 9 is consistent with the results.¹³ Capture of this ion pair by chloride gives the α -chloro amide product. The simple expedient of adding excess chloride ion (5 equiv) to the reaction mixture increases the capture efficiency and gives increased yields (yields in parentheses, eq 1). If no chloride ion is present, the ion pair capture by triethylamine gives salt 6. The use of other nucleophiles to capture 9 could lead to a general synthesis of 2-substituted secondary amides. We were delighted to find that treatment of both 5a and 5e with triethylamine and lithium bromide in dichloromethane gave 2-bromo amides 10a,e in high yields. Alternatively, treatment of 5a,e with triethylamine and water in acetonitrile gave 2-hydroxy amides 11a,e in high yields also (eq 2).



These results support the idea that nucleophilic capture of ion pairs produced from O-sulfonylated hydroxamic acids offers a very versatile route to 2-substituted amides. In contrast, Miller has recently suggested that an S_N2' pathway is followed in the reactions of sulfonyloxy β -lactams with nucleophiles.⁶ Studies

(12) The n -values for chloride and bromide are 4.37 and 5.79, respectively. Pearson, R. G.; Sobel, H.; Songstad, J. *J. Am. Chem. Soc.* **1968**, *90*, 319.

(13) It is also possible that an aziridinone (α -lactam) is formed from enolate 7. The α -lactam is a valence tautomer of ion pair 9. While an α -lactam cannot be specifically ruled out as the reactive intermediate, the efficient capture of weak nucleophiles like chloride under neutral conditions is more consistent with the ion pair as the reactive species. Lengyel, I.; Sheehan, J. C. *Angew. Chem., Int. Ed. Engl.* **1968**, *7*, 25.

are in progress to resolve these mechanistic issues and to fully explore the synthetic potential of these processes.

Acknowledgment. This work was supported by the National Science Foundation (9004980) and the National Institutes of Health (GM44529-01). B.W.K. is a participant in the MARC program sponsored by the National Institutes of Health.

Supplementary Material Available: Experimental details for preparations and experiments described in the text (5 pages). Ordering information is given on any current masthead page.

The Asymmetric Mixed-Valent Complex $\{[Mn(2-OH-3,5-Cl_2-SALPN)]_2(THF)\}ClO_4$ Shows a Temperature-Dependent Interconversion between $g = 2$ Multiline and Low-Field EPR Signals

Erlund Larson,¹ Alice Haddy,² Martin L. Kirk,³ Richard H. Sands,*² William E. Hatfield,*³ and Vincent L. Pecoraro*¹

*Departments of Chemistry and Physics and Biophysics
University of Michigan, Ann Arbor, Michigan 48109*

*Department of Chemistry
University of North Carolina
Chapel Hill, North Carolina 27599*

Received June 2, 1992

Considerable debate has focused on the origin of the $g = 2$ "multiline" and $g = 4.1$ EPR signals observed in the S_2 state of the photosynthetic oxygen-evolving complex.^{4,5} One explanation of these signals is that they arise from the ground and excited states of a single manganese cluster or from different spin states of a conformationally perturbed cluster.⁵ Mixed-valent Mn(II/III) dimers have shown temperature-dependent EPR signals.⁶ However, there are no examples where the strongly coupled Mn(III/IV)(μ_2 -O)₂ cores ($J = -120$ cm⁻¹) exhibit additional features beyond the 16-line spectrum of the $S = 1/2$ ground state.⁷ This is significant since it is believed that the S_2 multiline arises from a cluster containing Mn(III) and Mn(IV).⁸ Herein we report a highly asymmetric Mn(III/IV) dimer, 1, which has an exceptionally long Mn-Mn separation and weak antiferromagnetic coupling and provides the first observation of a reversible, thermally regulated transition from an $S = 1/2$ ground-state multiline to a low-field transition ($g \approx 5$) from an $S = 3/2$ first excited state. $\{[Mn^{III}(2-OH-3,5-Cl_2-(SALPN))]_2(MeOH)\}$, 2 (where 2-OH-3,5-Cl₂-(SALPN) = *N,N'*-bis(3,5-dichlorosalicylidene)-1,3-di-

(1) Department of Chemistry, University of Michigan.

(2) Department of Physics and Biophysics, University of Michigan.

(3) Department of Chemistry, University of North Carolina.

(4) Babcock, G. T.; Barry, B. A.; Debus, R. J.; Hoganson, C. W.; Atamain, M.; McIntosh, L.; Sithole, I.; Yocum, C. F. *Biochemistry* **1989**, *28*, 9557. Rutherford, A. W. *Trends Biochem. Sci.* **1989**, *14*, 227. Christou, G. *Acc. Chem. Res.* **1989**, *22*, 328. Pecoraro, V. L. *Photochem. Photobiol.* **1988**, *48*, 249. Wiegardt, K. *Angew. Chem., Int. Ed. Engl.* **1990**, *28*, 1153. Govindjee; Coleman, W. *J. Sci. Am.* **1990**, *262*, 50. Dismukes, G. C. *Photochem. Photobiol.* **1986**, *43*, 99. Hansson, O.; Aasa, R.; Vänngard, T. *Biophys. J.* **1986**, *51*, 825.

(5) (a) DePaula, J. C.; Beck, W. F.; Brudvig, G. W. *J. Am. Chem. Soc.* **1986**, *108*, 4002. (b) Kim, D. H.; Britt, D. R.; Klein, M. P.; Sauer, K. *J. Am. Chem. Soc.* **1989**, *112*, 9389.

(6) Chang, H. R.; Larsen, S. K.; Boyd, P. D. W.; Pierpont, C. G.; Hendrickson, D. N. *J. Am. Chem. Soc.* **1988**, *110*, 4565. Diril, H.; Chang, H. R.; Nilges, M. J.; Zhang, X.; Potenza, J. A.; Schugar, H. J.; Isied, S. S.; Hendrickson, D. N. *J. Am. Chem. Soc.* **1989**, *111*, 5102.

(7) Kirby, J. A.; Robertson, A. S.; Smith, J. P.; Thompson, A. C.; Cooper, S. R.; Klein, M. P. *J. Am. Chem. Soc.* **1981**, *103*, 5537.

(8) Guiles, R. D.; McDermott, A.; Yachandra, V. K.; Cole, J. L.; Dexheimer, S. L.; Britt, R. D.; Wiegardt, K.; Bossek, U.; Sauer, K.; Klein, M. P. *Biochemistry* **1990**, *29*, 471. George, G. N.; Prince, R. C.; Cramer, S. P. *Science* **1989**, *243*, 789. Penner-Hahn, J. E.; Fronko, R.; Pecoraro, V. L.; Bowlby, N. F.; Betts, S. D.; Yocum, C. F. *J. Am. Chem. Soc.* **1990**, *112*, 2549.

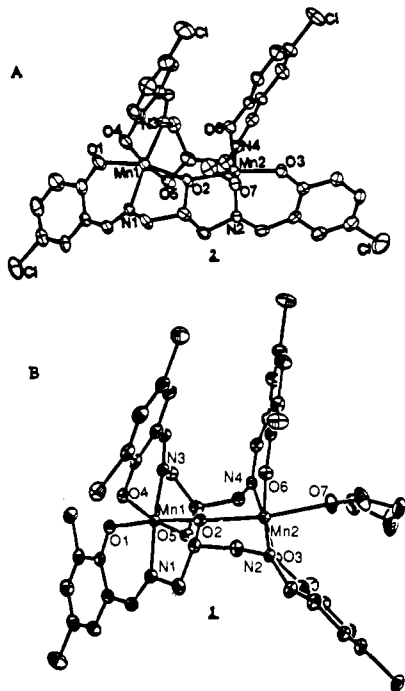


Figure 1. ORTEP diagrams of $[\text{Mn}^{\text{III/IV}}][2\text{-OH-3,5-Cl}_2(\text{SALPN})]_2(\text{MeOH})_2$, **2** (A) and $[\text{Mn}^{\text{III/IV}}][2\text{-OH-3,5-Cl}_2(\text{SALPN})]_2(\text{THF})_2$, **1** (B) with thermal ellipsoids at 30% probability. Important bond lengths (Å) and angles (deg) for **1**: Mn1–O1, 1.858 (4); Mn1–O2, 1.889 (4); Mn1–O4, 1.905 (4); Mn1–O5, 1.852 (4); Mn1–N1, 1.984 (6); Mn1–N3, 1.958 (6); Mn2–O2, 2.202 (3); Mn2–O3, 1.876 (4); Mn2–O6, 1.886 (4); Mn2–O7, 2.296 (4); Mn2–N2, 1.994 (5); Mn2–N4, 2.012 (6); Mn1–Mn2, 3.65; Mn1–O2–Mn2, 126.7 (2); O1–Mn1–O2, 171.5 (2); O1–Mn1–O4, 90.6 (2); O1–Mn1–O5, 92.6 (2); O1–Mn1–N1, 90.4 (2); O1–Mn1–N3, 92.5 (2); O2–Mn1–O4, 87.5 (2); O2–Mn1–O5, 90.6 (2); O2–Mn1–N1, 81.6 (2); O2–Mn1–N2, 95.8 (2); O4–Mn1–O5, 170.1 (2); O4–Mn1–N1, 97.0 (2); O4–Mn1–N3, 88.5 (2); O5–Mn1–N1, 92.4 (2); O5–Mn1–N3, 82.0 (2); N1–Mn1–N3, 173.7 (2); O2–Mn2–O3, 109.7 (2); O2–Mn2–O6, 82.1 (2); O2–Mn2–O7, 164.3 (2); O2–Mn2–N2, 77.0 (2); O2–Mn2–N4, 96.0 (2); O3–Mn2–O6, 166.9 (2); O3–Mn2–O7, 84.8 (2); O3–Mn2–N2, 87.6 (2); O3–Mn2–N4, 92.6 (2); O6–Mn2–O7, 83.0 (2); O6–Mn2–N2, 89.7 (2); O6–Mn2–N4, 91.8 (2); O7–Mn2–N2, 98.3 (2); O7–Mn2–N4, 89.2 (2); N2–Mn2–N4, 172.5 (2).

amino-2-hydroxypropane) is an asymmetric, monoalkoxide-bridged dimer which undergoes quasireversible electrochemical oxidation at +500 mV vs SCE in acetonitrile.⁹ Bulk electrolysis of **2** at +600 mV using NaClO_4 as supporting electrolyte gives the mixed-valence dimer $[\text{Mn}^{\text{III}}\text{Mn}^{\text{IV}}][2\text{-OH-3,5-Cl}_2(\text{SALPN})]_2(\text{THF})\text{ClO}_4$, **1**. X-ray quality crystals were obtained by slow evaporation from THF. The best model¹⁰ for **1** is illustrated as Figure 1. Previous valence-trapped, mixed-valent dimers have had highly symmetric ligand environments, whereas the polyhedra of Mn1 and Mn2 are strikingly different. The Mn2 polyhedron resembles the bis-salicylideneiminato tetragonal coordination in $\text{Mn}^{\text{III}}(\text{SALEN})\text{Cl}$ (where SALEN = *N,N'*-bis(salicylidene)-ethylenediamine).¹¹ The Mn1 has bis-meridional coordination

(9) Bonadies, J. A.; Kirk, M. L.; Kessissoglou, D. P.; Lah, M. S.; Hatfield, W. E.; Pecoraro, V. L. *Inorg. Chem.* **1989**, *28*, 2037. Bonadies, J. A.; Maroney, M. J.; Pecoraro, V. L. *Inorg. Chem.* **1989**, *28*, 2044.

(10) X-ray parameters for **1**: $[\text{Mn}^{\text{III}}\text{Mn}^{\text{IV}}][2\text{-OH-3,5-Cl}_2(\text{SALPN})]_2(\text{THF})\text{ClO}_4$, $\text{Mn}_2\text{C}_{38}\text{H}_{30}\text{N}_4\text{O}_{11}\text{Cl}_9$, MW 1147.4; crystal system, triclinic (*P*1); $a = 13.885$ (4), $b = 14.265$ (3), $c = 16.652$ (5) Å; $\alpha = 101.40$ (2)°, $\beta = 105.18$ (3)°, $\gamma = 104.20$ (2)°; $V = 2963$ (2) Å³; $Z = 2$; $d_{\text{obsd}} = 1.32$ gm/cm³, $d_{\text{calcd}} = 1.29$ gm/cm³; crystal dimensions, 0.21 × 0.32 × 0.15 mm; Mo K α (0.7107 Å); $T = 298$ K; Syntex P2₁ four-circle diffractometer; data were reduced using the SHELX program package; structure solved using SHELX86; complex atomic scattering factors were used in refinement;¹² carbon atoms of THF were refined isotropically. Hydrogen atoms were included at calculated positions with fixed *U* values (isotropic thermal parameters) of 0.08 Å²; $\mu = 8.7$ cm^{−1}; $5 < 2\theta < 45^\circ$; unique reflections = 7764, no. of parameters = 597; reflections with $I > 3\sigma(I) = 5979$; $R = 0.0935$, $R_w = 0.1035$. Anal. Calcd for $\text{Mn}_2\text{-C}_{38}\text{H}_{38}\text{N}_4\text{O}_{11}\text{Cl}_9$, MW 1219.5: C, 41.33; H, 3.12; N, 4.59; Cl, 26.20; Mn, 9.02. Found: C, 41.08; H, 3.14; N, 5.03; Cl, 26.07; Mn, 8.73.

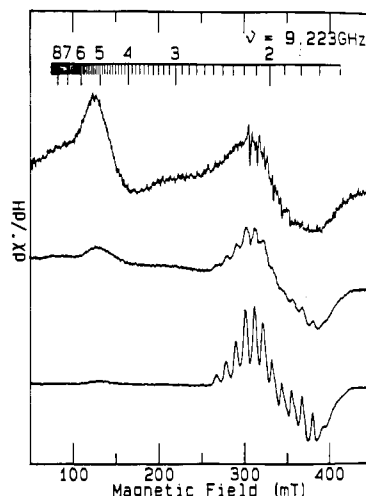


Figure 2. X-band (9.22 GHz) EPR spectra of **1** in DMF glass at 20 (bottom), 43 (middle), and 110 K (top).

from two ligand molecules, resulting in an isostructural coordination environment with $\text{Mn}^{\text{IV}}(\text{SALADHP})_2$, **3** (where SALADHP = *N*-salicylidene-2-amino-1,3-dihydroxypropane).¹² The Mn(IV/III) reduction of **1** occurs at +500 mV vs SCE, while the same reduction occurs at −460 mV vs SCE with **3**.¹¹ This illustrates how appending a metal to a bridging ligand can destabilize the Mn(IV) oxidation level by ~900 mV.

The Mn1–heteroatom distances observed in **1** are arranged in a nearly octahedral geometry. Four short and two long distances (having severe angular distortion) are seen for Mn2. In **2**, the Mn1 coordination sphere has an axial Jahn–Teller distortion along the O1–Mn1–O2 vector (Mn1–O1, 2.084 Å; Mn1–O2, 2.317 Å), and the corresponding axial elongation of Mn2 is along N4–Mn2–O7 (Mn2–N4, 2.291 Å; Mn2–O7, 2.334 Å). Oxidation to **1** results in significantly shorter Mn1–O1 (1.858 Å) and Mn1–O2 (1.889 Å) bonds and lengthening of the Mn2–O2 bond (1.202 Å vs 2.190 Å). The Jahn–Teller distortion in Mn2 shifts to the O2–Mn2–O7 vector, which is the only superexchange pathway between Mn1 and Mn2 in **1**. The Mn1–Mn2 separation of 3.65 Å is the longest yet reported for an Mn(III/IV) dimer.

Variable-temperature magnetic susceptibility data of **1** (2.6–100 K) were collected at 1 kOe in a region where the magnetization varied linearly with the applied field. The data indicated weak antiferromagnetism and were analyzed using Heisenberg exchange theory. The best fit values are $g = 2$ (fixed) and $J = -10$ cm^{−1}. The long Mn–Mn separation and the poor superexchange pathway ($d_{z^2-y^2}$ is a nonmagnetic orbital on Mn1) lead to weak magnetic exchange that is unprecedented for dioxo Mn(III/IV) dimers.

The X-band EPR spectrum of **1** at 20 K (Figure 2, bottom) shows a unique multiline EPR spectrum with approximately 12 lines centered around $g \approx 2$. Comparison of this signal with a 15-GHz spectrum (Figure 3, supplementary material) suggests significant g anisotropy. The spectrum can be approximated by $g_{\perp} = 2.01$, $g_{\parallel} = 1.93$, $A_{\text{Mn(III)}} \approx A_{\text{Mn(IV)}} = (103-112) \times 10^{-4}$ cm^{−1}. This compares to $g = 2.0075$, $A_{\text{Mn(III)}} = 144 \times 10^{-4}$ cm^{−1}, and $A_{\text{Mn(IV)}} = 76 \times 10^{-4}$ cm^{−1} for the Mn(III/IV) dimer of the *Lactobacillus plantarum* catalase.¹³ As the temperature is raised to 43 (Figure 2, middle) and 110 K (Figure 2, top), a new low-field feature at $g \approx 5$ develops. The bottom spectrum in Figure 2 is recovered when the sample temperature is again lowered to 20 K. We assign the low-field component to a thermally populated $S = 3/2$ first excited state of the dimer. This signal does not arise from an Mn(IV) impurity since complexes such as **3** show strong signal intensity at helium temperatures. Previous workers have suggested that the $g = 2$ multiline and $g = 4.1$ signals of the OEC

(11) Butler, W. M.; Pecoraro, V. L. *Acta Crystallogr.* **1986**, *C42*, 1151.

(12) Li, X.; Kessissoglou, D. P.; Butler, W. M.; Pecoraro, V. L. *Inorg. Chem.* **1987**, *26*, 2487.

(13) Fronko, R. M.; Penner-Hahn, J. E.; Bender, C. J. *J. Am. Chem. Soc.* **1988**, *110*, 7554.

might arise from thermal populations of ground- and excited-state manifolds. Complex 1 provides the first example of such behavior in a Mn(III/IV) model complex.

Acknowledgment. We thank Professor James Penner-Hahn for useful discussions and access to experimental data prior to publication. This work was supported by the National Institutes of Health (V.L.P., GM 39406; R.H.S., GM32785) and the National Science Foundation (W.E.H., CHE-8807498). The authors thank the Alfred P. Sloan Foundation for a fellowship to V.L.P., Amoco for a fellowship to E.L., the Program on Protein Structure and Design for a fellowship to A.H., and the office of the Vice President for Research for a grant to R.H.S.

Supplementary Material Available: Tables of fractional atomic coordinates, thermal parameters, bond distances, and bond angles for all atoms (Tables 1-4), P-band EPR spectrum of 1 at 20 K (Figure 3), and complete numbering scheme for 1 (Figure 4) (16 pages); table of observed and calculated structure factors (Table 5) (28 pages). Ordering information is given on any current masthead page.

Tailored Ligands for Asymmetric Catalysis: The Hydrocyanation of Vinylarenes

T. V. RajanBabu* and Albert L. Casalnuovo*

Contribution No. 6077, Du Pont Central Research and Development, Experimental Station, E328 Wilmington, Delaware 19880-0328

Received November 19, 1991

Despite the enormous progress made in enantioselective synthesis during the last decade, the development of asymmetric, metal-catalyzed carbon-carbon bond forming reactions remains a challenging area of research.¹ In this communication we report our initial findings on the asymmetric Markovnikov addition of HCN to vinylarenes in the presence of Ni(0) complexes of 1,2-diol phosphinites derived from readily available sugars.² The enantioselectivity of this reaction has been optimized by steric and electronic tuning of an easily modified ligand system (Figure 1), and ee's (enantiomeric excesses) up to 85% have been achieved. Vinylarenes constitute an important class of substrates for this reaction because the resulting 2-aryl-2-propionitriles are potential precursors for a variety of commercially important non-steroidal antiinflammatory agents.^{3,4} Historically, the only significant asymmetric inductions observed for this important carbon-carbon

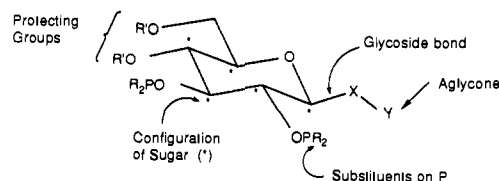
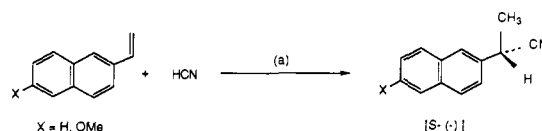


Figure 1. Tunable sites on a diol phosphinite ligand system.

bond forming reaction⁵ have been limited to norbornene derivatives,⁶ and the highest selectivity reported thus far is 40% ee for a low-yielding hydrocyanation of norbornene at 120 °C.^{6b,c}

Because of the current commercial importance of the well-known antiinflammatory drug naproxen, we chose 6-methoxy-2-vinylnaphthalene (MVN) and 2-vinylnaphthalene (2-VN) as prototypical substrates for our initial studies. Addition of HCN to these substrates, carried out according to the protocol in the equation below, gave the corresponding 2-naphthalene-2-propionitriles with unprecedented enantioselectivity.⁷ In sharp contrast to the well-known Pt-catalyzed carbonylation of vinylarenes,⁸ no trace of the linear product was detected under these conditions.^{8,9}



(a) 0.001 to 0.05 equiv [Ni(L)* to Ni]; 1.3-2.0; η
[Ni] = Ni(COD)₂; L* = 1,2-diolphosphinite

Initial screening of a variety of 1,2- and 1,3-diol phosphinites prepared from readily available mono- and disaccharides^{10a} indicated the overwhelming importance of the gluco configuration of the sugar backbone and the juxtaposition of a β -aryl *O*-glycoside (X-Y = *O*-aryl in Figure 1) for high enantioselectivity. While the steric and electronic manipulations of the aglycone (Y in Figure 1) yielded a modest, yet discernible, improvement on the

(3) Rieu, J.; Boucherle, A.; Cousse, H.; Mouzin, G. *Tetrahedron* **1986**, *42*, 4095-4131.

(4) Nugent, W. A.; McKinney, R. J. *J. Org. Chem.* **1985**, *50*, 5370-5372.

(5) Tolman, C. A.; McKinney, R. J.; Seidel, W. C.; Druliner, J. D.; Stevens, W. R. *Adv. Catal.* **1985**, *33*, 1-46.

(6) (a) Elmes, P. S.; Jackson, W. R. *Aust. J. Chem.* **1982**, *35*, 2041-2051.

(b) Hodgson, M.; Parker, D.; Taylor, R. J.; Ferguson, G. *Organometallics* **1988**, *7*, 1761-1766. (c) Baker, M. J.; Pringle, P. G. *J. Chem. Soc., Chem. Commun.* **1991**, 1292-1293.

(7) In a typical scouting reaction, a solution of Ni(COD)₂ (0.009 g, 0.033 mmol) in about 1 mL of benzene was added to a solution of the chiral ligand (0.042 mmol) in about 1 mL of benzene under an N₂ atmosphere, stirred for 30 min, and added to the vinylarene (0.65 mmol). The reaction mixture was brought to the specified temperature, and HCN (0.600 mL, 0.22 M in toluene, 0.13 mmol) was added by syringe or autopipet. The reaction mixture was analyzed by GC and HPLC after about 3-4 h of stirring. Yields typically ranged from 5 to 100%. ee's were determined (on a sample filtered through silica gel; ether/hexane) by HPLC using either a Daicel Chiralcel OJ or OB column: 5% *i*-PrOH/hexane, 1 mL/min, 40 °C. For MVN the faster eluting enantiomer was determined to be the *S* isomer by comparison to an enriched sample prepared from (*S*)-naproxen via dehydration of the amide. In preparative runs with the best catalysts (entries 4a,b), up to 2.5 equiv of HCN and 0.1-1.0 mol % of Ni was used in appropriate solvents and the product (>85% yield) was isolated by column chromatography. Optically pure (*S*)-(-)-6-methoxy-2-naphthalene-2-propionitrile (mp 99-100 °C; >99% ee; $[\alpha]_D^{25} = -28.4^\circ$, *c* 1, CHCl₃) may be prepared by two recrystallizations of enriched (75-85% ee) nitrile using ether/hexanes as the solvent system. (See supplementary material for details.)

(8) Stille, J. K.; Su, H.; Brechot, P.; Parrinello, G.; Hegedus, L. S. *Organometallics* **1991**, *10*, 1183-1189 and references cited therein.

(9) For solutions to the regiochemical problem, see: (a) Alper, H.; Hamel, N. *J. Am. Chem. Soc.* **1990**, *112*, 2803-2804. (b) Amer, I.; Alper, H. *J. Am. Chem. Soc.* **1990**, *112*, 3674-3676. (c) Brown, J. M.; Cook, S. J.; Khan, R. *Tetrahedron* **1986**, *42*, 5105.

(10) (a) These include phosphinites from galactose, fructofuranose, lactose, and trehalose. The importance of the sugar backbone is evident from the low ee's observed upon using bis[3-(trifluoromethyl)phenyl]phosphinite from *R*-binaphthol and (*S,S*)-1,2-*trans*-cyclohexanediol (32 and 7% ee respectively for 6-methoxy-2-vinylnaphthalene). For a more complete list, see supplementary material. (b) See supplementary material.

(1) For recent reviews, see: (a) Hayashi, T.; Kumada, M. In *Asymmetric Synthesis*; Morrison, J. D., Ed.; Academic Press: New York, 1985; Vol. 5, pp 147-169. (b) Bosnich, B. *Asymmetric Catalysis*; Martinus Nijhoff Publishers: Dordrecht, The Netherlands, 1986. (c) Brunner, H. *Synthesis* **1988**, 645-654. (d) Ojima, I.; Clos, N.; Bastos, C. *Tetrahedron* **1989**, *45*, 6901-6939. (e) Brown, J. M.; Davies, S. G. *Nature* **1989**, *342*, 631-636. (f) Noyori, R. *Science* **1990**, *248*, 1194-1199. (g) Pfaltz, A. *Chimia* **1990**, *44*, 202-213. For a discussion of the importance of chirality in pharmaceutical industry, see: Borman, S. *Chem. Eng. News* **1990**, July 9, 9-14.

(2) The use of phosphinites has so far been largely limited to hydrogenation of dehydro amino acids. See, for example: (a) Cullen, W. R.; Sugi, Y. *Tetrahedron Lett.* **1978**, 1635-1636. (b) Selke, R. *React. Kinet. Catal. Lett.* **1979**, *10*, 135-138. (c) Jackson, R.; Thompson, D. J. *J. Organomet. Chem.* **1978**, *159*, C29-C31. (d) Johnson, T. H.; Rangarajan, G. *J. Org. Chem.* **1980**, *45*, 62-65. (e) Jackson, W. R.; Lovel, C. G. *Aust. J. Chem.* **1982**, *35*, 2069-2075. (f) Selke, R.; Pracejus, H. *J. Mol. Catal.* **1986**, *37*, 213-225. (g) Habus, I.; Raza, Z.; Sunjic, V. *J. Mol. Catal.* **1987**, *42*, 173-181. (h) Selke, R.; Hauptke, K.; Krause, H. W. *J. Mol. Catal.* **1989**, *56*, 315-328.